European Spine Journal (2019) 28:710–718
https://doi.org/10.1007/s00586-018-5839-y

ORIGINAL ARTICLE

A mouse model for the study of transplanted bone marrow mesenchymal stem cell survival and proliferation in lumbar spinal fusion

Ioan A. Lina[1] · Wataru Ishida[2] · Jason A. Liauw[2] · Sheng-fu L. Lo[2] · Benjamin D. Elder[3] · Alexander Perdomo-Pantoja[2] · Debebe Theodros[2] · Timothy F. Witham[2] · Christina Holmes[2]

Received: 16 April 2018 / Revised: 21 October 2018 / Accepted: 25 November 2018 / Published online: 3 December 2018

Abstract

Purpose Bone marrow aspirate has been successfully used alongside a variety of grafting materials to clinically augment spinal fusion. However, little is known about the fate of these transplanted cells. Herein, we develop a novel murine model for the in vivo monitoring of implanted bone marrow cells (BMCs) following spinal fusion.

Methods A clinical-grade scaffold was implanted into immune-intact mice undergoing spinal fusion with or without freshly isolated BMCs from either transgenic mice which constitutively express the firefly luciferase gene or syngeneic controls. The in vivo survival, distribution and proliferation of these luciferase-expressing cells was monitored via bioluminescence imaging over a period of 8 weeks and confirmed via immunohistochemistry. MicroCT imaging was performed 8 weeks to assess fusion.

Results Bioluminescence imaging indicated transplanted cell survival and proliferation over the first 2 weeks, followed by a decrease in cell numbers, with transplanted cell survival still evident at the end of the study. New bone formation and increased fusion mass volume were observed in mice implanted with cell-seeded scaffolds.

Conclusions By enabling the tracking of transplanted bone marrow-derived cells during spinal fusion in vivo, this mouse model will be integral to developing a deeper understanding of the biological processes underlying spinal fusion in future studies.

Graphical abstract These slides can be retrieved under Electronic Supplementary Material.

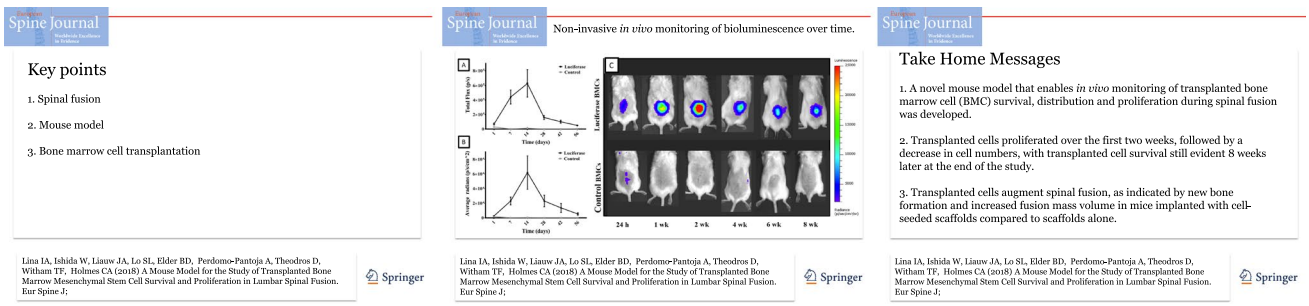

Keywords Spinal fusion · Mouse model · Bone marrow · Luciferase · Mesenchymal stem cell

Introduction

Spinal fusion surgery is an increasingly common procedure used in the treatment of spinal pathology. Clinically, autologous bone marrow aspirate containing a heterogeneous

Electronic supplementary material The online version of this article (https://doi.org/10.1007/s00586-018-5839-y) contains supplementary material, which is available to authorized users.

Extended author information available on the last page of the article

population of cells, including mesenchymal stem cells (MSCs), has been successfully used with a variety of grafting materials to augment spinal fusion procedures [1, 2]. Indeed, recent studies have demonstrated that both concentrated and unconcentrated bone marrow aspirate in combination with clinical bone grafting materials can enhance interbody and posterolateral fusion outcomes, in some cases achieving rates similar to autograft bone [3]. Furthermore, many pre-clinical and clinical fusion studies have expanded to explore the use of allogenic and/or in vitro culture-expanded bone marrow MSCs, including several phase II/III clinical trials examining the use of allogeneic marrow-derived MSCs [3, 4]. Although these cell-based therapies have generally proved successful in promoting fusion, much remains to be learned about the fate of transplanted cells and their interactions with host cells.

While bone marrow and MSC transplantation studies in pre-clinical bone regeneration models have generally yielded enhanced bone formation [5–7], results have varied depending upon the transplantation site, delivery method, and/or experimental model under investigation. Most research tracking the survival of transplanted bone marrow-derived cells has employed xenotransplantation, immune-compromised host animals and/or ex vivo culture-expanded cells, thus presenting several key limitations. In the case of spinal fusion studies, the survival and fate of donor cells have largely gone unanalyzed. There is thus a crucial need for more clinically relevant models to enable detailed research into the survival and fate of transplanted donor cells in bone regeneration, particularly in the context of spinal fusion.

The mouse lumbar fusion model provides a wide range of analytical research tools, including numerous transgenic strains [8–10]. Utilizing donor cells from transgenic mice that constitutively express a marker gene enables non-invasive cell tracking, thus circumventing many of the disadvantages of exogenous labeling methods, while also allowing for the use of immune-intact hosts. Developed by Cao et al., the transgenic mouse line FVB-Tg(CAG-luc,-GFP) L2G85Chco/J expresses luciferase throughout most tissues under the ubiquitous CAG promoter [11], and has been used in a number of transplantation studies to trace various cell and tissue types [12]. Bone marrow-derived cells from FVB-Tg(CAG-luc,-GFP)L2G85Chco/J mice have exhibited strong luciferase expression and have been used in transplantation studies to trace hematopoietic reconstitution as well as MSC engraftment in the myocardium [13].

In this study, we developed a clinically oriented mouse model of lumbar fusion to study the fate of transplanted bone marrow cells (BMCs) during spinal fusion. Our model employs the transplantation of freshly isolated BMCs from FVB-Tg(CAG-luc-GFP)L2G85Chco/J donor mice alongside a clinical-grade bone graft substitute into syngeneic FVB/NJ host mice, thus enabling the non-invasive in vivo tracking of transplanted BMC survival, distribution and proliferation over time within the fusion space via bioluminescence imaging (BLI).

Materials and methods

Animals and reagents

This study was approved by the Animal Care and Use Committee at the Johns Hopkins University School of Medicine. Donor FVB-Tg(CAG-luc,-GFP) L2G85Chco/J mice were obtained from the Jackson Laboratory (Bar Harbor, Maine, USA) and bred in house. Host FVB/NJ mice were also obtained from the Jackson Laboratory. Vitoss® bone graft substitute was purchased from Stryker (Kalamazoo, MI, USA). D-luciferin was purchased from Gold Biotechnology (St. Louis, MO, USA). Vectastain Elite ABC Kit (Goat IgG), Avidin/Biotin Blocking Kit, and Vectastain DAB Kit were purchased from Vector Laboratories (Burlingame, CA, USA). Anti-luciferase antibody (no. 200-103-150S) was purchased from Rockland Immunochemical (Gilbertsville, PA, USA).

Surgical technique

Six-to-eight-week-old female FVB/NJ mice underwent posterolateral lumbar spinal fusion surgery and were divided into three experimental groups: (1) Vitoss® bone graft substitute scaffold alone ($n = 10$); (2) Vitoss® seeded with control FVB/NJ bone marrow cells (BMCs) ($n = 15$); or, (3) Vitoss® seeded with syngeneic BMCs isolated from FVB-Tg(CAG-luc,-GFP)L2G85Chco/J mice ($n = 15$). Recipient mice were anesthetized via intraperitoneal (IP) injection of ketamine (90 mg/kg) and xylazine (10 mg/kg). The surgical site was shaved and prepped with 70% ethanol and betadine. A 15-mm dorsal midline incision from the L1 vertebrae to the posterior superior iliac spine was made. After placing a retractor, a second incision was made through the dorsolumbar fascia to expose the paravertebral muscles. Paraspinous muscles were dissected away from midline with a size 15 scalpel blade. Both the inferior and superior articular processes of the L5–L6 facet joints were then decorticated using a pneumatic 0.7-mm burr. Approximately 2.5 mm^3 of Vitoss® grafting material, with or without seeded BMCs, was placed at the L5–6 junction and the retractor was removed. Fascia and skin were closed in layers with 5-0 absorbable sutures (Polysorb, Medtronic, Minneapolis, MN, USA). In addition to the main experimental groups listed above, supplementary groups of mice were implanted with either luciferase-expressing BMCs ($n = 12$) or control BMCs ($n = 12$), solely to obtain three samples at each time point for immunohistochemical analysis.

Bone marrow cell extraction

6- to 8-Week-old female FVB/NJ or FVB-Tg(CAG-luc-GFP) L2G85Chco/J donor mice were euthanized and bilateral femurs and tibias were isolated, dissected and cleaned in a sterile biological safety cabinet. Bone marrow was flushed using a syringe with a 25-gauge needle and sterile phosphate buffered saline (PBS). The resulting bone marrow suspension was passed through a 100-µm nylon mesh filter and subsequently underwent hemolysis and centrifugation. Recovered nucleated cells were enumerated, re-suspended and seeded onto Vitoss® scaffolds (2.5 million cells per scaffold per side) prior to implantation. Cellular isolation was performed concurrently with surgical exposure to ensure that isolated cells were implanted 20–30 min following seeding to maintain cellular viability.

Bioluminescence imaging

Mice implanted with either luciferase-expressing BMCs or control BMCs were imaged at 24 h and at 1-, 2-, 4-, 6- and 8-week postoperatively via the IVIS® Spectrum pre-clinical imaging system (PerkinElmer, Waltham, MA, USA). Imaging was performed 10 min after IP injection of 10 µL/g of D-luciferin (15 mg/ml in saline) with an exposure time of 5 min. Mice were anesthetized via inhalation of an isoflurane–O_2 gas mixture. The total bioluminescence radiance/flux (photons/s), area (cm^2), and average bioluminescence signal (photons/s/cm^2) were measured for each mouse at each time point using Living Image Software (Caliper LifeSciences, PerkinElmer). The data were then averaged for each group. The difference in bioluminescent flux signal (p/s) and average bioluminescence (p/s/cm^2) at 24-h post-transplantation between cell implantation groups was analyzed using a standard *T* test.

MicroCT imaging

Mice were imaged at a resolution of 100 µm at 8-week postoperatively tilizing a NanoSPECT/CT (Bioscan). Mice were anesthetized via inhalation of an isoflurane–O_2 gas mixture. Axial cross-sections were generated to quantitatively calculate fusion mass volume via ImageJ software (US National Institutes of Health, Bethesda, MD) as previously described [14].

Histology and immunohistochemistry

At 1-, 2-, 4- and 8-week postoperatively, lumbar spines were harvested, fixed overnight in 4% paraformaldehyde, decalcified in 14% ethylenediaminetetraacetic acid for 4 weeks, dehydrated by ethanol series, and embedded in paraffin. Serial sections (10 µm thick) were cut, deparaffinized in xylene, and subsequently rehydrated. Adjacent sections of each fusion mass were assessed via immunohistochemical staining for luciferase expression and via hematoxylin and eosin (H&E) staining, alcian blue staining, and Masson's trichrome staining for formation of bone, cartilage, osteoid and blood vessels. Immunohistochemical staining was performed using the Vectastain Elite ABC Kit. Sections were treated with 0.05% w/v citraconic anhydride in PBS for 30 min at 95 °C for antigen retrieval, and with 1% w/v H_2O_2 in DPBS for 20 min to inhibit endogenous peroxidase activity. Slides were subsequently incubated overnight at 4 °C in blocking solution (normal rabbit serum, 5% w/v bovine serum albumin, and 0.2% w/v sodium azide (Sigma)), followed by avidin/biotin blocking (via a Vector Laboratories kit). Sections were incubated overnight at 4 °C with the primary luciferase antibody (diluted 1:1000 in PBS with normal rabbit serum, 5% w/v bovine serum albumin, 0.2% w/v sodium azide, and 0.1% Tween 20), followed by incubation with the secondary biotinylated rabbit anti-goat IgG antibody for 60 min at room temperature, and incubation with the peroxidase-conjugated biotin–avidin complex for 30 min at room temperature. Finally, staining with a 3,30-diaminobenzidine (DAB) kit was performed according to manufacturer's instructions.

Statistical methods

Comparison of bioluminescence flux signals (photons/s) at 24-h post-implantation between luciferase-expressing and control BMCs was performed via the Mann–Whitney test, as not all flux data groups passed the Shapiro–Wilk normality test. Average fusion mass volumes were compared via the Kruskal–Wallis test and group comparisons were made via Dunn's multiple comparisons test, as not all data groups passed the Shapiro–Wilk normality test. All statistical analysis was performed using GraphPad Prism software (GraphPad Software Inc, CA).

Results

In vivo monitoring and ex vivo detection of transplanted luciferase-expressing cells

Mice recovered well from surgery and did not exhibit any significant complications. However, 3 of the 15 mice transplanted with luciferase-expressing cells died from anesthesia overdose during repeated imaging and were thus excluded from analyses. Imaging of mice transplanted with luciferase-expressing BMCs revealed a significant increase in bioluminescence flux signal (photons/s) and average bioluminescence signal (photons/s/cm^2) over the initial 2-week period following surgery, suggesting cellular proliferation, followed by a decrease in signal from 4 through 8 weeks, likely

representing transplanted cell death (Fig. 1). The greatest increase in signal (> 500%) was observed between 24-h and 1-week postoperatively. Looking at BLI signal over time for each mouse (Fig. 2), the peak flux signal was reached at varying points, with approximately 33% (4/12) of the mice exhibiting maximum bioluminescence at week 1, 58% (7/12) at week 2, and 8% (1/12) at week 4. This individual-to-individual difference was unrelated to the use of different donor mice. Interestingly, mice transplanted with control BMCs displayed a bioluminescence signal at 24 h, albeit at significantly lower levels ($p < 0.001$). However, from 1 week onwards, mice transplanted with control BMCs exhibited no significant signal.

Correlating with BLI data, immunohistochemical staining displayed the highest number of luciferase-positive cells within the fusion masses at weeks 1 and 2 (Fig. 3). Interestingly, at week 2, many luciferase-positive cells were also identified on the surface of the host lamina adjacent to the

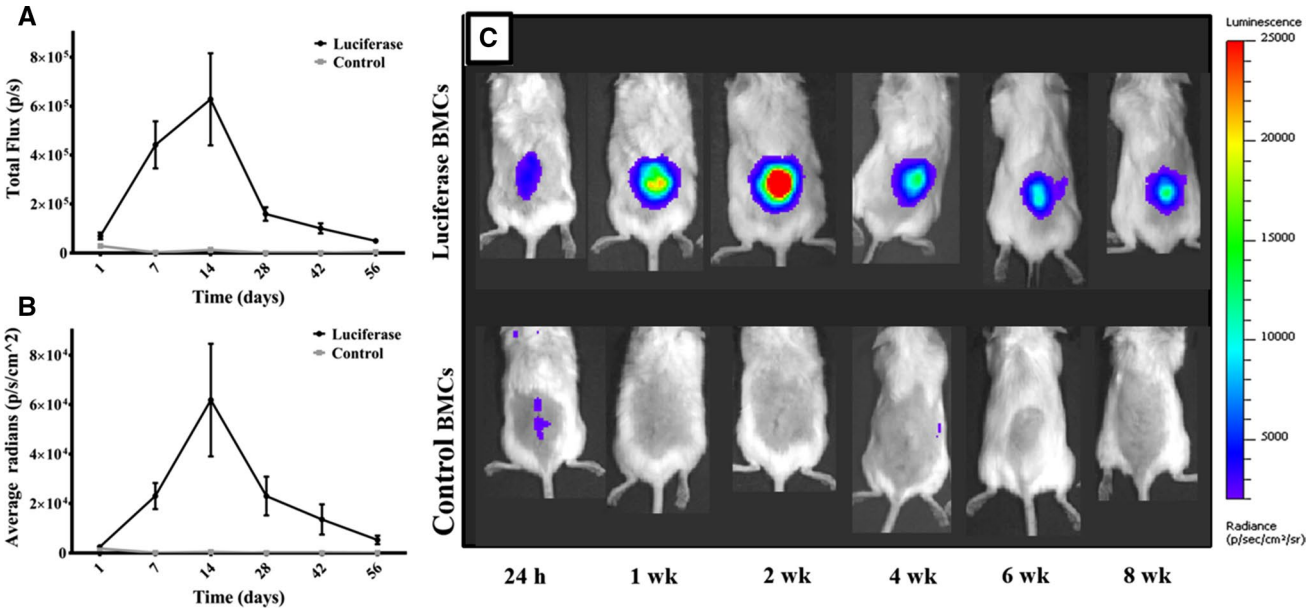

Fig. 1 Non-invasive in vivo monitoring of bioluminescence over time. **a** Average total flux signal (p/s) over time for mice implanted with syngeneic luciferase-expressing BMSCs (black line, $n = 12$) or control syngeneic BMSCs (gray line, $n = 15$). **b** Average bioluminescence signal, normalized for the size of the bioluminescent area (radians = p/s/cm^2), over time for mice implanted with syngeneic luciferase-expressing BMSCs (black line, $n = 12$) or control syngeneic BMSCs (gray line, $n = 15$). **c** Representative images of bioluminescence signal over time for mice implanted with syngeneic luciferase-expressing BMSCs (top) or control syngeneic BMSCs (bottom)

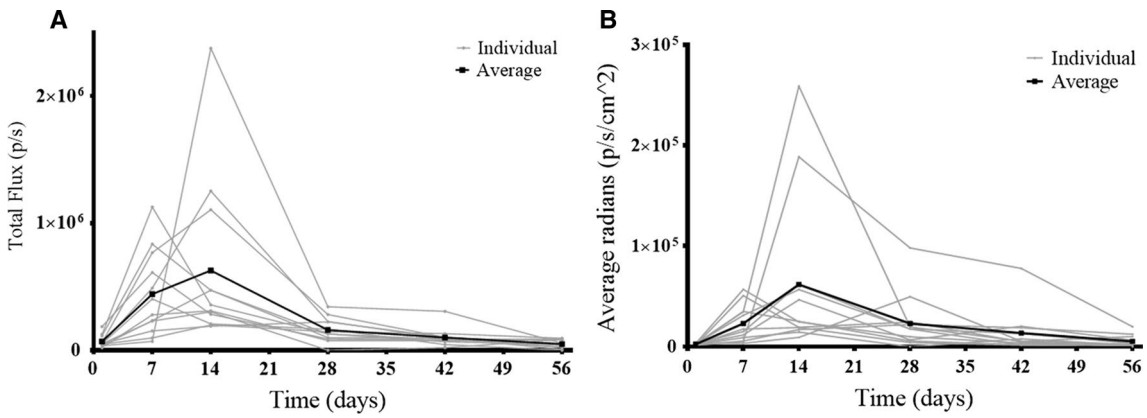

Fig. 2 Bioluminescence imaging of individual mice implanted with syngeneic luciferase-expressing BMSCs over time. **a** Total flux signal (p/s) over time for each individual mouse in the study (gray line) in comparison with the overall average signal (black line). **b** Average bioluminescence signal, normalized for the size of the bioluminescent area (radians = p/s/cm^2), over time for each individual mouse in the study (gray line) in comparison with the overall average signal (black line)

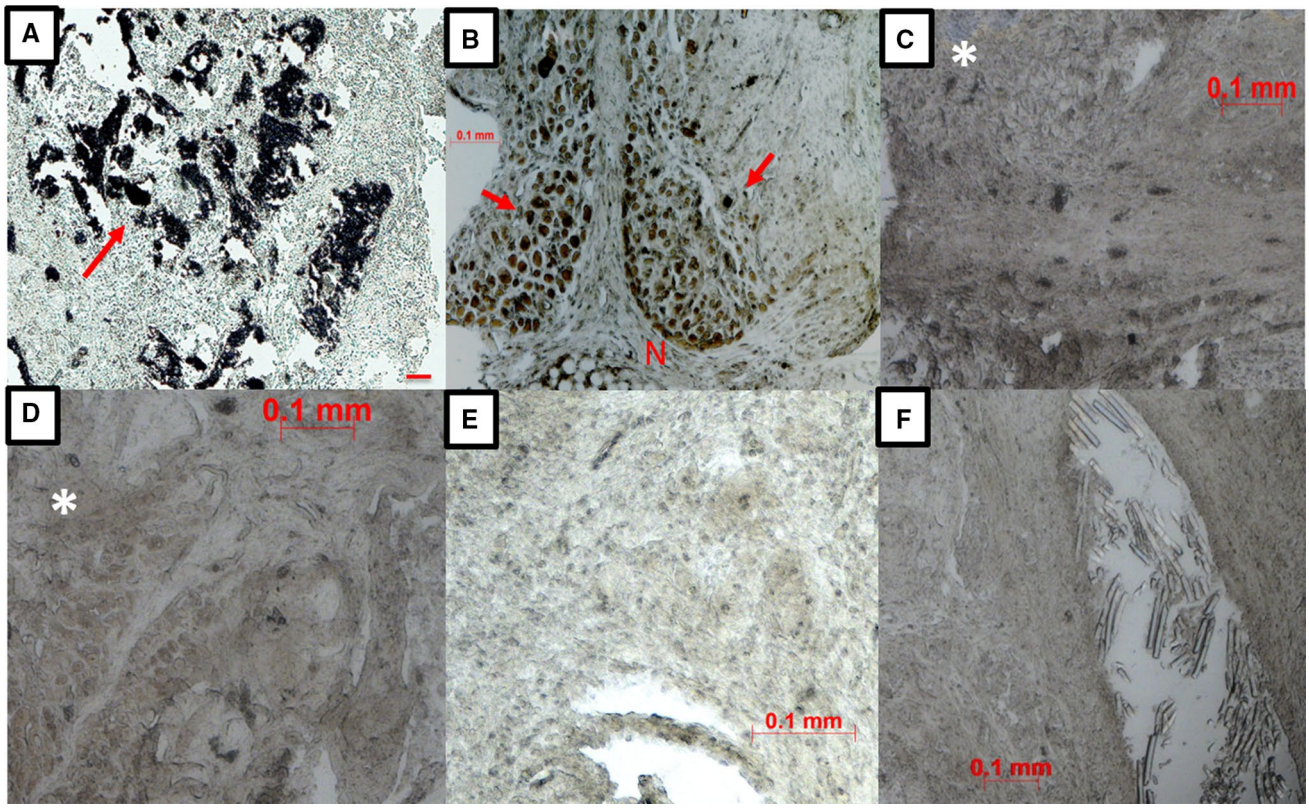

Fig. 3 Representative images of immunohistochemical staining for luciferase-positive cells within the fusion mass over time. Low-magnification images: **a** week 1, abundant luciferase-positive cells were identified within the scaffold (10×, arrow); **b** week 2: many luciferase-positive cells were identified on the surface of a native lamina (25×, arrow). Higher magnification images within the fusion mass and scaffold: **c** week 2 (100×); **d** week 4 (100×); **e** week 8 (100×); and, **f** negative control at week 2 (100×). Scale bars in each image represent 100 µm. *N* native lamina, *F* fusion mass

fusion mass (Fig. 3b). The number of luciferase-positive cells decreased significantly at week 4 (Fig. 3d) and week 8 (Fig. 3e), as was observed with BLI. No staining for luciferase-positive cells was observed in mice implanted with control cells at any time point (Fig. 3f).

Fusion mass evaluation

Histological staining of cell-implanted groups revealed the presence of osteoid, cartilage, bone marrow and microvasculature within the fusion bed at week 2 (Fig. 4a–e). At week 4, the amount of bone tissue within the fusion bed increased, with some surrounding cartilage and osteoid (Fig. 4f–h). By week 8, the fusion mass between the native facet joints developed into mature bone extremely similar to the adjacent host bone, and also contained bone marrow and cartilage with evidence of bone remodeling (Fig. 4i–k).

MicroCT imaging at week 8 (Fig. 5) showed that the fusion masses in mice implanted with cells were generally more radiopaque than those implanted with scaffolds alone (Fig. 5d–f), suggesting more bone formation. This apparent increase in radiodensity was also more uniformly spread throughout the fusion masses in the cell-implanted groups, compared to the patchier pattern of radiopaque spots in mice with scaffolds alone, thus suggesting improved fusion. More importantly, mice implanted with cells displayed significantly higher fusion mass volumes than those implanted with scaffolds alone ($p = 0.002$) (Fig. 5g). As expected, no statistically significant differences in fusion mass volume were observed between mice implanted with luciferase-expressing and control BMCs ($p = 0.709$).

Discussion

By employing freshly isolated BMCs from FVB-Tg(CAG-luc,-GFP)L2G85Chco/J mice and a clinical-grade carrier, our model closely mirrors the current clinical practice of utilizing carriers seeded with bone marrow aspirate in spinal fusion. This is the first study to describe an animal spinal fusion model that allows for the tracking of unpassaged, minimally manipulated BMCs during fusion. By avoiding the use of immunocompromised rodents, transfected cells or culture-expanded cells, our model also maintains the

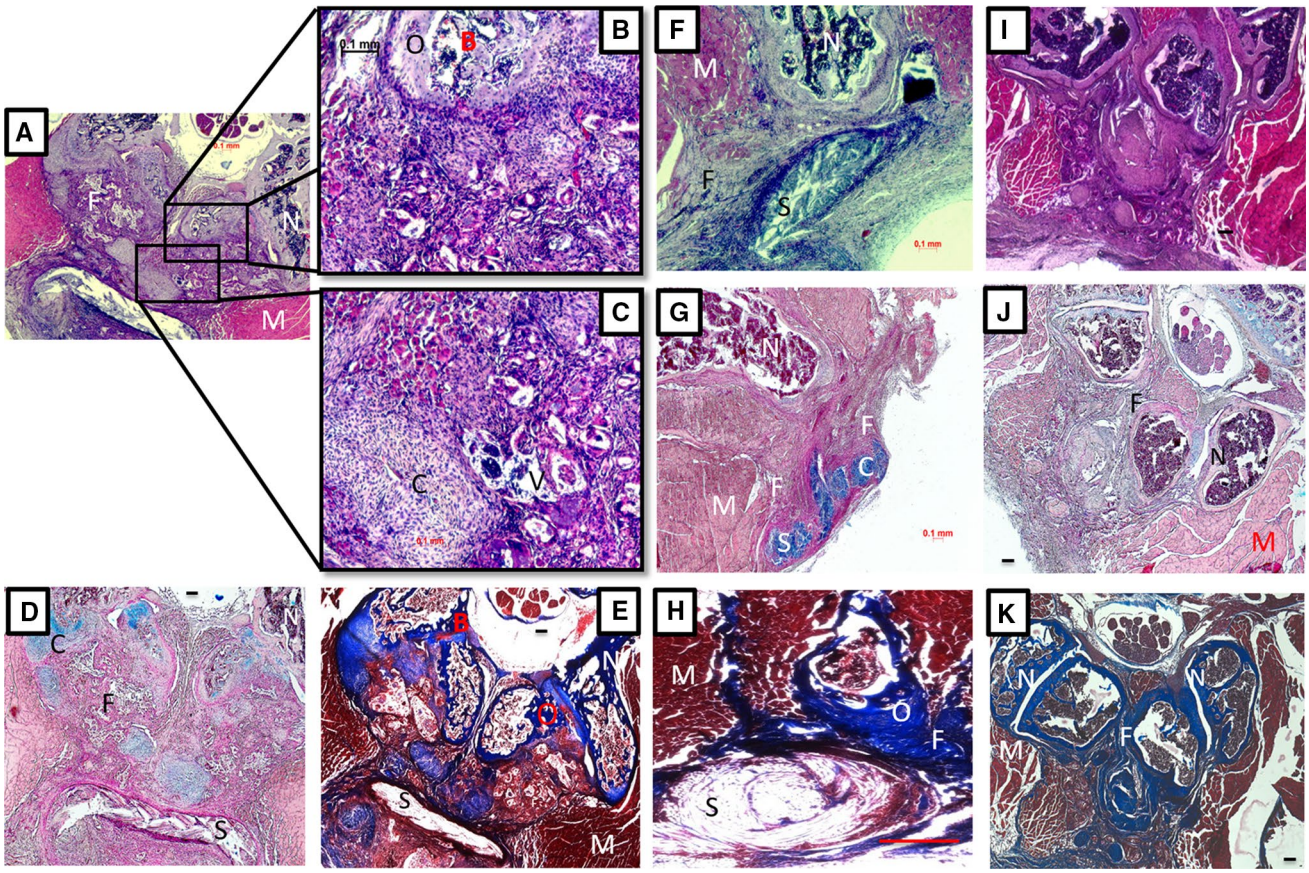

Fig. 4 Representative histological images of the fusion mass over time. Week 2: **a** H&E staining; **b** higher magnification (100×) inset image displaying osteoid from image "a"; **c** higher magnification (100×) inset image displaying cartilage and microvasculature from image "a'; **d** alcian blue staining, confirming the presence of cartilage and osteoid (25×). **e** Masson's trichrome staining (25×). Week 4: **f** H&E staining (40×); **g** alcian blue staining (25×); **h** Masson's trichrome staining (100×). Week 8 **i** H&E staining (40×); **j** alcian blue staining (25×); and, **k** Masson's trichrome staining (25×). Scale bars in each image represent 100 µm. *B* bone marrow, *C* cartilage, *F* fusion mass, *M* muscle, *N* native lamina, *O* osteoid, *S* scaffold, *V* microvessel

native healing processes that are clinically relevant to bone regeneration.

In this study, the BLI signal from transplanted BMCs increased significantly at the fusion site over the first 2 weeks, and then decreased to similar levels as observed 24-h post-transplantation by 6 weeks. However, BLI signal and thus cell survival were detectable for the entire 8-week duration of the study. This differs significantly from previous transplantation studies which showed poor cell survival in immune-intact mice (Table 1). In an ectopic implantation study, for example, Qiao and colleagues observed that the BLI signal from transplanted MSCs decreased continuously over the 4-week study period [15]. Similarly, Huang and colleagues observed a steadily decreasing BLI signal from MSCs locally injected in a femoral fracture model, lasting only 14-day post-injection [16]. Meanwhile, in the only other study to track transplanted cells in spinal fusion, the BLI signal from luciferase-transduced goat MSCs increased from day 1 to day 7, followed by a dramatic decrease to negligible levels by day 21 in an immunocompromised rat model [17]. The increased early proliferation and prolonged cell survival observed in the present study compared to previous research may be due to the heterogeneous nature of the fresh bone marrow aspirate used. Future studies will employ co-staining for various hematopoietic cell and mesenchymal stem cell surface markers to determine exactly which subpopulations of transplanted cells survive and proliferate in vivo.

In this study, the increased fusion mass volumes observed in the cell-seeded groups indicated that the transplanted BMCs augmented bone formation and fusion. In contrast, in the immunocompromised rat fusion study tracking luciferase-expressing MSCs, no bone formation was observed [17]. As significant numbers of transplanted BMCs did not persist past week 3, the resulting enhancement in fusion mass volume may primarily be due to early paracrine interactions with host cells, such as immunomodulation. Future studies will determine whether these paracrine effects are the main contributor to increased bone formation or whether

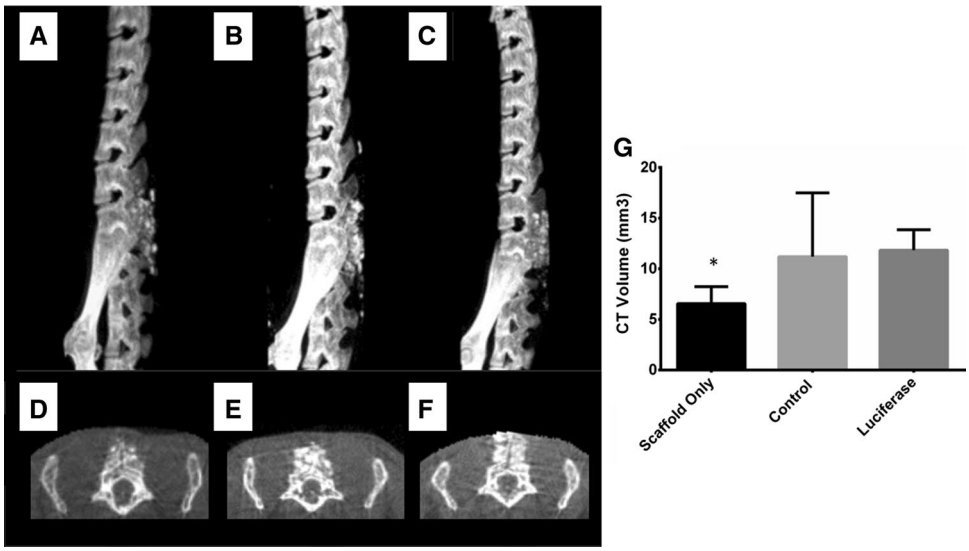

Fig. 5 CT fusion evaluation 8-weeks postoperatively. Representative sagittal and axial microCT images, respectively, of mice implanted with: **a**, **d** Vitoss scaffolds alone; **b**, **e** scaffolds seeded with syngeneic control BMSCs; and, **c**, **f** scaffolds seeded with syngeneic luciferase-expressing BMSCs. **g** Average fusion mass volume at 8-weeks postoperatively as determined via microCT image analysis for mice implanted with: Vitoss scaffolds alone (black bar), scaffolds seeded with syngeneic control BMSCs (light gray bar), and scaffolds seeded with syngeneic luciferase-expressing BMSCs (dark gray bar). Data presented as mean ± std ($n = 9$ for scaffold alone, $n = 14$ for control BMSCs, $n = 12$ for luciferase BMSCs) *($p = 0.04$) versus control; and ($p < 0.01$ vs. luciferase)

transplanted cells also directly form bone. Additionally, studies are currently under way to further enhance fusion outcomes in our model via optimization of BMC number as well as using the intertransverse process fusion model.

The use of BLI to track transplanted cell fate in vivo is widespread due to its high sensitivity, noninvasiveness and low toxicity, as well as its ability to enable longitudinal and quantitative cell monitoring [18, 19]. In this study, the observation of a BLI signal 24-h postoperatively in mice transplanted with control BMCs was surprising and may have been due to the presence of elevated levels of acute inflammatory enzymes at the operative site thus leading to non-luciferase-mediated oxidation of the luciferin substrate. Previous studies utilizing luciferase-expressing cells to track transplanted MSCs in osteogenic contexts have yielded differing results depending upon experimental design factors such as whether cells were transduced with a luciferase reporter, the method of transduction, the design of the luciferase-reporter plasmid, whether cells were xenogenic and the species involved, the passage number of the transplanted cells, the site of delivery, the method of delivery, and the type of carrier used [15–17, 20, 21] (Table 1). For example, in two ectopic transplantation studies utilizing luciferase-transduced xenogenic MSCs in immunocompromised mice, one, employing goat MSCs, observed a dramatic BLI signal increase from days 7 to 21 [17], while the other, employing human MSCs, observed a continuous BLI signal decrease, with the most significant loss (85%) over the first 15 days [20]. However, such immunocompromised animal models may not give a true indication of transplanted cell fate due to the important roles played by immune cells in bone healing and remodeling.

Conclusions

The mouse model developed in this study enabled non-invasive in vivo tracking of transplanted BMC survival, distribution and proliferation over time within the fusion space in the most clinically relevant context to date, and exhibited prolonged cell proliferation and survival compared to other osteogenic transplantation models. Further optimization of this model will enable the detailed study of the roles played by transplanted BMCs and MSCs compared to host cells during spinal fusion. Furthermore, this mouse model will provide an important tool for the evaluation of the cellular mechanisms underlying fusion as well as the effects of various fusion treatments on transplanted cell survival, proliferation and differentiation.

Funding Work in the Spinal Fusion Laboratory is supported by The Gordon and Marilyn Macklin Foundation and the AO Foundation (Grant No. S-16-59H).

Compliance with ethical standards

Conflict of interest The authors declare that they have no conflict of interest.

Table 1 Recent studies tracking transplanted luciferase-expressing BMCs in osteogenic animal models

Study/reference	Cell transplantation details	Animal model	Bioluminescence imaging protocol and results	Other notable results
Current study	Freshly isolated BMCs from transgenic CAG-*luc* mouse strain Seeded on a VITOSS scaffold (Stryker)	Mouse (FVB/NJ) Spinal fusion	Imaging at 1, 2, 4, 6 and 8 wks BLI ↑ first 2 wks, rapid ↓ through 8 wks Peak signal: 14 d	Transplanted cells enhanced bone formation
Geuze et al. [17]	P1 goat BMCs Cryopreserved before and after lentiviral transduction with a *luc* reporter Seeded onto BCP particles (Progentix) and cultured 24 h	Immunocomp. Mouse (RAG-2-/- γc-/-Balb/c) Subcu. implant, 0.1, 0.5, 1×10^6 cells Immunocomp. Rat (nude Harlan Sprague–Dawley) [A]: Subcu. implant, 1×10^6 cells [B]: Spinal fusion, 3×10^6 cells	Imaging at 1 d, then weekly Mouse: BLI ↑ first 3 wks, gradual ↓ through 6 wks Peak signal: 21 d Rat [A]: BLI ↑ first 7 d, rapid ↓ through 7 wks Peak signal: 7 d Rat [B]: BLI ↑ first 7 d, rapid ↓ through 3 wks Peak signal: 7 d	Mouse: some bone formation Rat [A] & [B]: no bone formation
Todeschi et al. [21]	[A]: P1–P2 human BMCs [B]: P1–P2 human umbilical cord cells Transduced via retrovirus with a *luc* reporter 2.5×10^6 cells seeded onto SKELITE scaffold (Millenium Biologix)	Immunocomp. Mouse (CD1 nu/nu) Subcu. implantat	Imaging at 1, 7, 21, and 30 d [A]: BLI expression stable throughout study Peak signal: BLI not quantified [B]: continuous BLI ↓ with no signal by 30 d Peak signal: 1 d	[A]: bone formed [B]: no bone formed
Huang et al. [16]	P4-P8 BMCs from transgenic CMV-*luc* mouse strain [A]: 1×10^5 cells systemic injection (intracardiac) [B]: 1×10^5 cells local injection (femur)	Mouse (FVB/NJ) Femoral fracture	Imaging at 10 min, then every 2 d until signal disappears [A]: BLI detectable at fracture site starting at 5–8 d, lasting 1–3 d Peak signal: not quantified [B]: BLI continuous ↓ through 12–14 d Peak signal: 10 min	Transplanted cells enhanced bone formation at fracture site [A] & [B]: no significant difference
Manaserro et al. [20]	P3 human BMCs P1 cells transduced via lentivirus with a *luc* reporter and cryopreserved at P3 1×10^6 cells seeded onto BIOCORAL scaffold (Inoteb)	Immunocomp. Mouse (NMRI-nu) [A]: Subcu. implant [B]: Femoral defect	Imaging at 1 d, then 2×wk for 5 wks, then weekly through 10 wks [A]: BLI continuous ↓ (85% by 15 d) Peak signal: 1 d [B]: BLI continuous ↓ (85% by 15 d) Peak signal: 1 d	Transplanted cells enhanced bone formation [B] formed more bone than [A]
Qiao et al. [15]	P3 BMCs from transgenic β-actin-*luc* mouse strain 1×10^6 cells seeded in MATRIGEL	Mouse (FVB/NJ) Subcu. implant	Imaging at 0,1, 3, 5, 7, 14, 21, 28, and 35 d BLI ↑ 1 d, continuous ↓ Peak signal: 1 d	Addition of IGF enhanced BLI at 21–35 d, however, ≪ 1 d

BCP, biphasic calcium phosphate; BLI, bioluminescence imaging signal; BMCs, bone marrow cells; d, day(s); hr, hour (s); Immunocomp., immunocompromised; *luc*, luciferase; Subcu., subcutaneous; wk, week

References

1. Kitchel SH (2006) A preliminary comparative study of radiographic results using mineralized collagen and bone marrow aspirate versus autologous bone in the same patients undergoing posterior lumbar interbody fusion with instrumented posterolateral lumbar fusion. Spine J 6:405–411. https://doi.org/10.1016/j.spinee.2005.09.013
2. Neen D, Noyes D, Shaw M et al (2006) Healos and bone marrow aspirate used for lumbar spine fusion: a case controlled study comparing healos with autograft. Spine (Phila Pa 1976) 31:E636–E640. https://doi.org/10.1097/01.brs.0000232028.97590.12
3. Salamanna F, Sartori M, Brodano GB et al (2017) Mesenchymal stem cells for the treatment of spinal arthrodesis: from preclinical research to clinical scenario. Stem Cells Int 2017:1–27. https://doi.org/10.1155/2017/3537094

4. Robbins MA, Haudenschild DR, Wegner AM, Klineberg EO (2017) Stem cells in spinal fusion. Glob Spine J 7:801–810. https://doi.org/10.1177/2192568217701102
5. Grayson WL, Bunnell BA, Martin E et al (2015) Stromal cells and stem cells in clinical bone regeneration. Nat Rev Endocrinol 11:140–150. https://doi.org/10.1038/nrendo.2014.234
6. Undale AH, Westendorf JJ, Yaszemski MJ, Khosla S (2009) Mesenchymal stem cells for bone repair and metabolic bone diseases. Mayo Clin Proc 84:893–902. https://doi.org/10.1016/S0025-6196(11)60506-5
7. Šponer P, Kučera T, Diaz-Garcia D, Filip S (2014) The role of mesenchymal stem cells in bone repair and regeneration. Eur J Orthop Surg Traumatol 24:257–262. https://doi.org/10.1007/s00590-013-1328-5
8. Bobyn J, Rasch A, Little DG, Schindeler A (2013) Posterolateral inter-transverse lumbar fusion in a mouse model. J Orthop Surg Res 8:2. https://doi.org/10.1186/1749-799X-8-2
9. Rao RD, Bagaria VB, Cooley BC (2007) Posterolateral intertransverse lumbar fusion in a mouse model: surgical anatomy and operative technique. Spine J 7:61–67. https://doi.org/10.1016/j.spinee.2006.03.004
10. Kolind M, Bobyn JD, Matthews BG et al (2015) Lineage tracking of mesenchymal and endothelial progenitors in BMP-induced bone formation. Bone 81:53–59. https://doi.org/10.1016/j.bone.2015.06.023
11. Cao Y-A, Wagers AJ, Beilhack A et al (2004) Shifting foci of hematopoiesis during reconstitution from single stem cells. Proc Natl Acad Sci USA 101:221–226. https://doi.org/10.1073/pnas.2637010100
12. Cao Y-A, Bachmann MH, Beilhack A et al (2005) Molecular imaging using labeled donor tissues reveals patterns of engraftment, rejection, and survival in transplantation. Transplantation 80:134–139
13. Sheikh AY, Lin S-A, Cao F et al (2007) Molecular imaging of bone marrow mononuclear cell homing and engraftment in ischemic myocardium. Stem Cells 25:2677–2684. https://doi.org/10.1634/stemcells.2007-0041
14. Lina IA, Puvanesarajah V, Liauw JA et al (2014) Quantitative study of parathyroid hormone (1-34) and bone morphogenetic protein-2 on spinal fusion outcomes in a rabbit model of lumbar dorsolateral intertransverse process arthrodesis. Spine (Phila Pa 1976) 39:347–355. https://doi.org/10.1097/brs.0000000000000169
15. Qiao H, Zhang R, Gao L et al (2016) Molecular imaging for comparison of different growth factors on bone marrow-derived mesenchymal stromal cells' survival and proliferation in vivo. Biomed Res Int 2016:1–10. https://doi.org/10.1155/2016/1363902
16. Huang S, Xu L, Sun Y et al (2015) The fate of systemically administrated allogeneic mesenchymal stem cells in mouse femoral fracture healing. Stem Cell Res Ther 6:206. https://doi.org/10.1186/s13287-015-0198-7
17. Geuze RE, Prins H-J, Öner FC et al (2010) Luciferase labeling for multipotent stromal cell tracking in spinal fusion versus ectopic bone tissue engineering in mice and rats. Tissue Eng Part A 16:3343–3351. https://doi.org/10.1089/ten.TEA.2009.0774
18. Welsh DK, Kay SA (2005) Bioluminescence imaging in living organisms. Curr Opin Biotechnol 16:73–78. https://doi.org/10.1016/j.copbio.2004.12.006
19. Kim JE, Kalimuthu S, Ahn B-C (2015) In vivo cell tracking with bioluminescence imaging. Nucl Med Mol Imaging (2010) 49:3–10. https://doi.org/10.1007/s13139-014-0309-x
20. Manassero M, Paquet J, Deschepper M et al (2016) Comparison of survival and osteogenic ability of human mesenchymal stem cells in orthotopic and ectopic sites in mice. Tissue Eng Part A 22:534–544. https://doi.org/10.1089/ten.tea.2015.0346
21. Todeschi MR, El Backly R, Capelli C et al (2015) Transplanted umbilical cord mesenchymal stem cells modify the in vivo microenvironment enhancing angiogenesis and leading to bone regeneration. Stem Cells Dev 24:1570–1581. https://doi.org/10.1089/scd.2014.0490

Affiliations

Ioan A. Lina[1] · Wataru Ishida[2] · Jason A. Liauw[2] · Sheng-fu L. Lo[2] · Benjamin D. Elder[3] · Alexander Perdomo-Pantoja[2] · Debebe Theodros[2] · Timothy F. Witham[2] · Christina Holmes[2]

✉ Christina Holmes
christinaa.holmes@gmail.com; cholmes19@jhmi.edu

[1] Department of Otolaryngology, The Johns Hopkins University School of Medicine, Baltimore, MD, USA

[2] Department of Neurosurgery, The Johns Hopkins University School of Medicine, 1550 Orleans St, Rm 2M-51, Baltimore, MD 21287, USA

[3] Department of Neurological Surgery, Mayo Clinic School of Medicine, Rochester, MN, USA